

# Experimental sediment wave morphologies – insights into complex flow behaviour at submarine channel margins.

I. Kane, W. D. McCaffrey & J. Peakall

*Institute of Geological Sciences, School of Earth and Environment, University of Leeds, Leeds, UK*

**ABSTRACT:** Complex palaeocurrents recorded from recent and ancient submarine channel-levee sands and sandstones have generally been interpreted to form in response to topographic deflection of overspilling flows. Physical modelling of overspilling sediment-laden turbidity currents within a curved channel model produced overbank sediment waves, with complex morphologies. Wave morphologies were linked to the generation of horizontal vortices at the channel-overbank transition, these were advected out from the channel causing entrained flow to be fully reversed with respect to the ‘normal’ overspill direction. Long-recognised from flooded fluvial compound channels, vortices are interpreted to form in response to shear stress imparted on the rapidly decelerating overbank fluid by the denser, faster-moving channelised flow. By tracking flow trajectories from video recordings it is evident that vortices within overspilling flow could account for the sediment wave morphologies and that this complex flow behaviour could account for palaeocurrent complexity within submarine channel-levee turbidites.

## 1 INTRODUCTION

Highly-variable palaeocurrents have been recorded from submarine channel levees in the subsurface and from ancient submarine channel levees at outcrop. In the levees of the Amazon Fan considerable ‘swing’ of palaeocurrents was recorded within individual turbidite beds, which was attributed by Hiscott et al. (1997, p.64) to “shifting patterns of meandering streamlines in the flow as deposition proceeds”. Kane et al. (2007), studying the master-bounding levee of a submarine channel-complex within the Upper Cretaceous Rosario Formation, noted that levee sandstones exhibit channel-axis parallel to convergent palaeocurrents on the inside of the levee crest; beyond the crest palaeocurrents are at first parallel to slightly divergent from the channel-axis, then with increasing distance from the crest, palaeocurrents become seemingly randomly oriented in the most channel-distal areas (Kane et al., 2007).

Experiments performed by Sellin (1964) showed that vortices formed over the margins of a submerged open channel during overbank flow. Zheleznyakov (1971) determined that as the relative depth of overbank flow increased, the strength and size of vortices diminished; similar conclusions were reached by other workers (e.g., Barishnikov et al. 1971; Bousmar & Zech, 1999; Prooijen et al., 2005). Myers and Brennan (1990) found that turbulence and vorticity generated at overspilling channel

margins increased flow velocities on the overbank area whilst decreasing channel flow velocities. Other workers have noted that turbulence intensity increases significantly at the interface between shallower and deeper areas of flooded fluvial channels, again these authors report increased turbulence developing from the margin and spreading outwards (Alavian & Chu, 1985; Tamai et al. 1986; Knight & Shiono, 1990; Knight et al., 1994; Shiono & Knight, 1991; Fukuoka & Watanabe, 1996, 1997; Naish & Sellin, 1996; Sofialdis & Prinos, 1999; Rowinski et al., 2002). The importance of mixing across channel-overbank transitions in compound channels has been investigated both numerically (e.g., Nokes and Hughes, 1994; Shiono et al., 2003) and physically (Wood and Liang, 1989; Shiono and Feng, 2003; Rowiński et al., 2005). Numerical modelling has allowed the large scale motion of these vortices to be resolved (Nadaoka & Yagi, 1998; Ikeda et al. 2002).

The experiments reported here represent the continuation of some earlier work by Kane et al. (2008) on intra-channel deposition within subaqueous channels; during those experiments, intricate extra-channel deposit morphologies were produced. The results and analysis of those and further experiments are presented here; the complex morphologies of overbank deposits are linked back to the nature of the overspilling flows and the generation of channel margin vortices.

## 1.1 Methodology

The experiments were performed in a flume tank 1.5 m deep, 1.7 m long, and 1.7 m wide. The tank has a false floor suspended 0.52 m above the tank floor, and an inlet channel 0.45 m wide that enters the tank on one side; the false floor extends into the channel (Fig. 1). A moat surrounds the false floor to create a sump preventing reflections and allowing maintenance of the density contrast between the dense current and the ambient fluid. To prepare an experimental run, suspensions are poured into a lock-release box with a closed vertical gate and an impeller with an electric drill attachment is used to thoroughly mix the suspension immediately prior to release. The lock-release box feeds into a 1.5 m long, 150 mm wide, straight channel, which in turn feeds into a continuous radius, curved channel model. The channel models comprise individual acrylic sheets with an identical channel cut-out (Fig. 1). These can be stacked to vary channel depth whilst maintaining a horizontal overbank area. Channel depth was systematically varied from 6 to 30 mm, at 6 mm increments, giving aspect ratios from 25 to 5 (henceforth referred to as ar25, ar12, ar8, ar6, ar5), equivalent to a wide range of natural systems, e.g., the Indus A (aspect ratio 27, Kenyon et al., 1995), to the Arguello (aspect ratio 5, EEZ-Scan Scientific Staff, 1988). No axial slope was employed.

The suspension was created using equal parts of two non-cohesive sediment analogues: spherical glass beads and crushed silica flour, mixed with tap-water, giving an initial sediment concentration of 5% by volume ( $1082 \text{ kg}^{-3}$ ) and a nominal grain-size distribution of  $1.8 \mu\text{m}$  ( $D_{10}$ ),  $27.3 \mu\text{m}$  ( $D_{50}$ ), and  $58.9 \mu\text{m}$  ( $D_{90}$ ). Experimental modelling attempts to reconstruct key elements of a natural system and obtain data to enable better understanding of that system.

## 1.2 Generic modelling approach

Here a generic modelling approach is adopted in order to recreate a reasonable process similarity to a prototype submarine channel, an approach which has been utilised successfully in fluvial modelling (e.g., Eaton and Church, 2004; Peakall et al., 2007). A degree of dynamic similarity is achieved by maintaining the Froude number for the model at approximately the same value as in the prototype, (e.g., Graf, 1971), and the flow Reynolds number within the fully turbulent flow field, i.e., Reynolds number  $>2000$  (e.g., Leeder, 1982). This generic modelling approach, while not scaling all variables such as discharge and concentration (currently unknown for submarine channels), has along with simpler analogue models, proven to be a powerful tool for un-

derstanding sedimentary systems (e.g., Schumm et al., 1987; Peakall et al., 1996, 2007; Tal and Paola, 2007). Representative values for the flow Reynolds number and the densimetric Froude number of flows entering the model were calculated as  $5.6 \times 10^3$  and 0.59 respectively. Estimates from the Amazon (Pirmez and Imran, 2003) and the Northwest Atlantic Mid-Ocean Channel (Klaucke et al., 1997) suggest Froude numbers between 0.4 and 0.8 respectively.

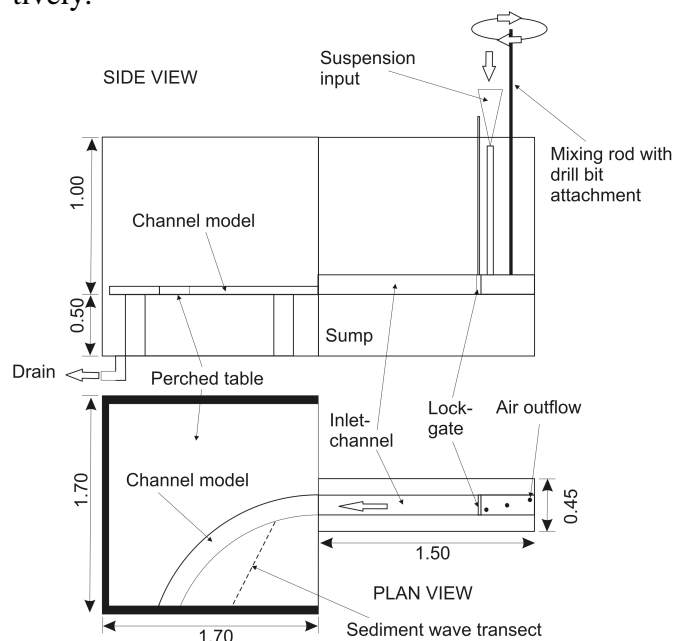


Figure 1. Experimental setup. The plan view (bottom) shows the channel model configuration and the location of the sediment wave profiles illustrated in Fig. 7. Measurements in metres

## 1.3 Measurement techniques

A video camera mounted above the tank was used to record the apparent flow path of overspilling sediment-laden currents. The deposit morphology was measured using a Teledictor Ultrasonic depth gauge (Best & Ashworth, 1994). Velocity profiles were taken within the channel using ultrasonic Doppler velocity profilers (UDVP, see Best et al., 2001) mounted at heights of 5, 13, 21, 29, 42 and 56 mm with the transmitters and receivers facing upstream, oriented horizontally and parallel to the local channel margins. Data were collected at three equally spaced points along the channel center line (P1 = proximal; P2 = medial; P3 = distal); a separate flow was run for each, as the probes are intrusive downstream of the measurement point.

## 2 EXPERIMENTAL RESULTS

### 2.1 Flow morphology and advance

A single flow was run in each of the channel models. Overspill was greater in the shallowest of the models

and progressively decreased as the channel depth was increased. Velocity profiles taken within the channel using UDVP, show a steady decline in the downchannel velocity; these are time averaged over 10 seconds and illustrate the characteristic velocity of the body of the flow (Fig. 2). Outlines of the flow head at 2 second intervals were extracted from the video data and illustrate the rapid lateral spreading of the flow as it exits the confinement of the input channel (Fig. 3).

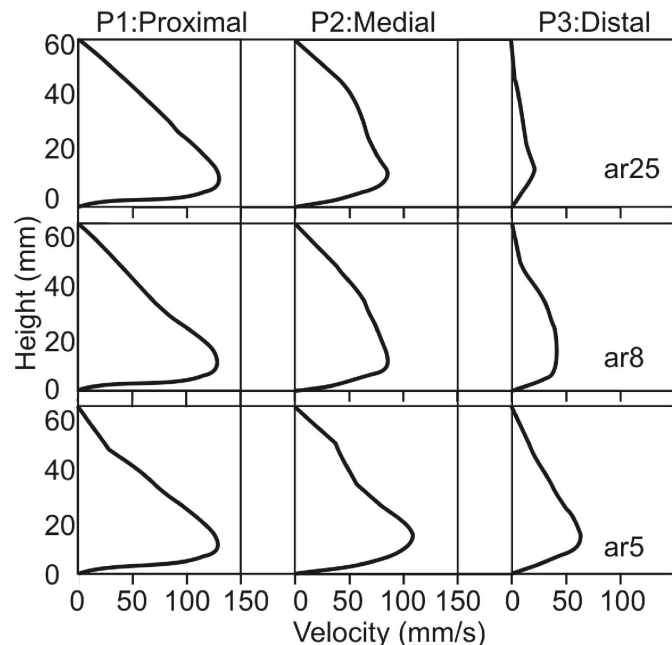


Figure 2. Velocity profiles from the ar25, ar8 and ar5 models ('ar' = aspect ratio). Velocity is maintained for greater distances downchannel in the channels with lower aspect ratios as less sediment is lost to the overbank area (compare to Fig. 3).

The spacing of the flow-head contours from the mid-depth (ar8) channel show an initial decrease in flow velocity, followed by a slight increase in velocity, particularly within the channel. In broad terms, stream lines diverge on the overbank area beyond the channel outer-bend and converge on the overbank area beyond the inner-bend; despite this, velocity is greater on the outer-bend overbank than on the inner-bend due to enhanced overspill at the channel outer-bend. A sequence of still-frames taken from the overhead video recordings more clearly showed the evolution of the flow and the direction of flow within the body. Flow vectors, on the outer-bend overbank, within the body of the flow and even toward the head of the flow were observed to show significant variation to the general direction of flow head propagation. Along the channel outer-bend margin, large-scale, coherent vortices with sub-vertical axes were observed to form, usually in the form of a large vortex which formed in the early stages of flow and vortices of decreased size produced as the flow waned (Fig. 4). Vortices did not appear to form in the shallowest of the models (ar25) but as the aspect ratio was decreased, resulting in a greater degree of flow confinement, vorticity became

more prevalent. In the deeper channels (ar8-ar5) a zone of overbank flow, extending overbank a couple of millimetres, was observed to follow the path of the channelised flow.

Along the channel inner-bend margin, vortices were not observed to form from flows within any of the channel models, i.e., inspection of the video recordings and still frames did not show any large-scale complex flow behaviour, flow vectors appeared to be approximately perpendicular to the advance of the flow head (Fig. 4).

## 2.2 Deposit morphology

The deposit profiles (Fig. 5) show ridge-like topographies which are aligned at variable angles to assumed flow-directions (Figs. 3 & 4). On the inner-bend overbank the flow head advance is generally aligned with the lunate crests of the ridges, i.e., the flow vectors are perpendicular to the crests of the deposits (Figs. 4 & 5). The inner-bend deposit crests have smaller radii than that of the channel inner-bend. On the outer-bend the deposit crests near to the channel are relatively straight-crested, but with increasing distance from the channel the features become more arcuate but curved away from the channel and apparently perpendicular to flow head position time contours. Towards the most-distal part of the outer-bend overbank the deposits exhibit the most complexity, generally showing three dominant alignments (Fig. 5). Morphologies generally become more intricate as the channel depth increases (Fig. 5).

## 2.3 Flow controls on deposit morphology

Where overspill diverges from the path of channelised flows its velocity decreases rapidly and the resulting cross-flow velocity gradient is inferred to create a shear layer inducing the formation of vortices with sub-vertical axes which amplify and spin out from the channel. Such phenomena are well known from open channel flows but have not been documented from subaqueous channels. In submarine channels a similar process of shear-coupling was hypothesised to account for the 'towing' of dilute supra-levee flow by the lower, denser, faster-moving channelised part of the flow (Peakall et al., 2000). The deeper channels are associated with the production of larger diameter, longer lived vortices; which may be related to the greater confinement depths promoting velocity maintenance within the channel (see Kane et al., 2008) and hence exerting greater shear stresses on the overbank portion of the flow. This kind of vortex formation may be viewed as a type of Kelvin-Helmholtz instability.

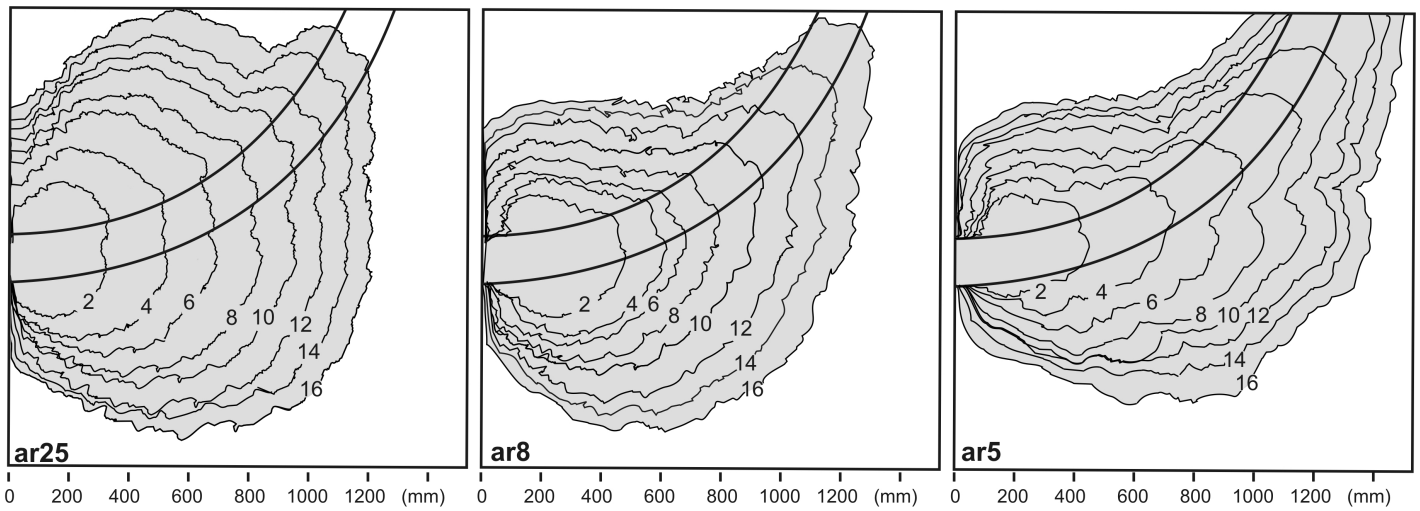


Figure 3. Propagation of the flow head within the shallowest (ar25), mid-depth and deepest channels ('ar' = aspect ratio), contours are numbered at 2 second intervals. Note that the deepest channel (ar5) exert much more control on the flow and maintains its velocity downchannel. Note the most forward position of the flow head varies from the inner-bend in the shallowest channel to the outer-bend in the deepest channel.

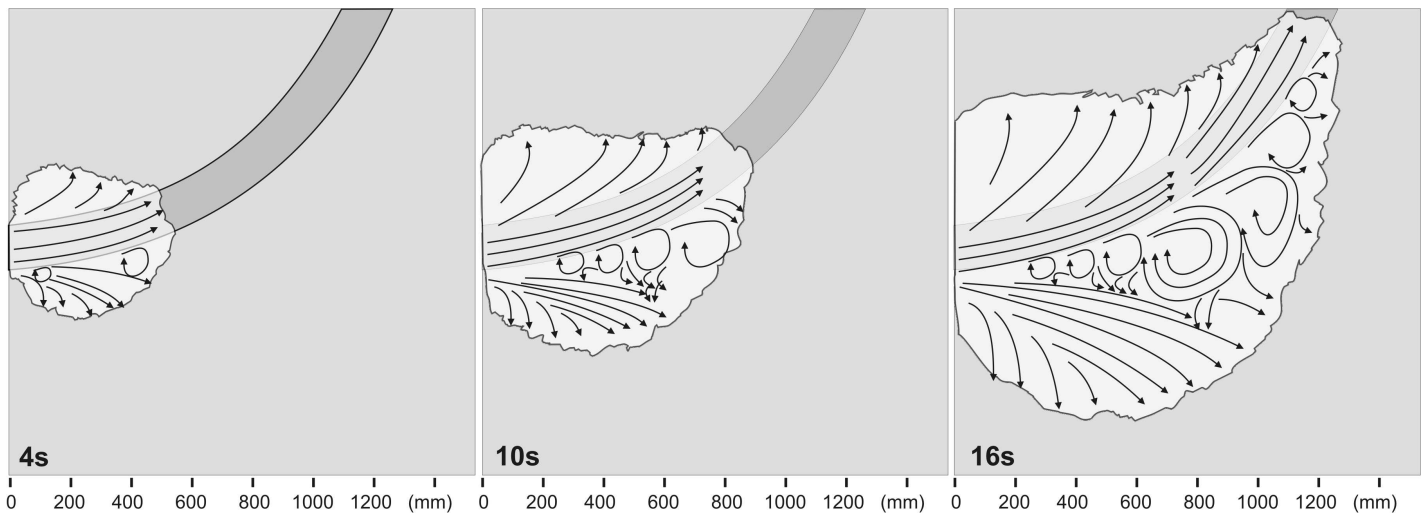


Figure 4. Outline of the flow head advance within the mid-depth (ar8) channel at 4, 10 and 16 seconds. Flow lines traced from stills of the overhead videos illustrate the complex behaviour of the body flow. Vortices form from the early stages on the outer-bend channel margin, growing laterally as the flow propagates over the overbank area. The vortices are interpreted to be a type of Kelvin Helmholtz instability generated by a shear layer that forms between the deeper, denser, faster moving channelised flow and the more dilute rapidly decelerating overbank flow.

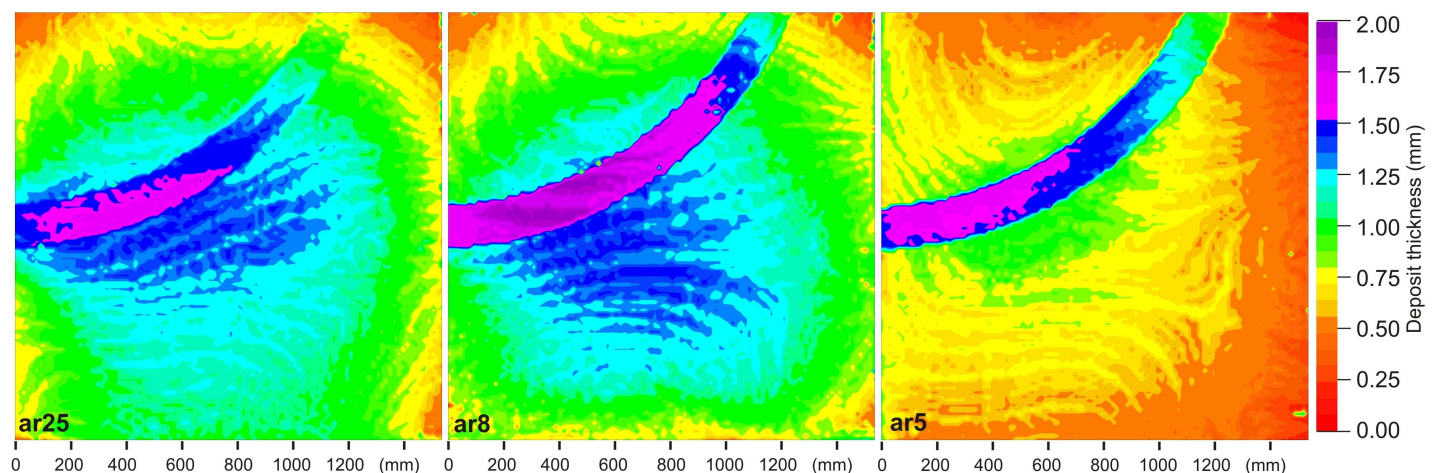


Figure 5. Deposit profiles after individual flow events within the shallowest (ar25), mid-depth and deepest channels. Note that the inner-bend morphology generally remains similar for all channel models whilst the outer-bend deposit morphology becomes increasingly complex as the channel model becomes deeper. The deposits are thought to represent sediment waves, their increasing complexity is related to the increased effect of vortex formation in the deeper channels in response to the greater shear stress exerted by faster moving flows

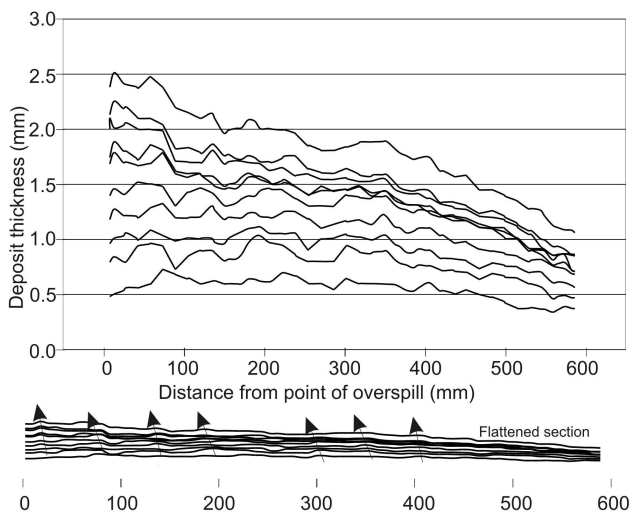


Figure 6. Sediment wave profiles from flows 1-10, run successively over the mid-depth (ar8) channel. The position of the transect is given in Fig. 1. The position of sediment waves is visible but to enable visualisation of the crest migration, the profiles are flattened (bottom); a component of upstream migration is clearly visible, suggesting an origin as lee waves formed from subcritical flows.

Sellin (1964) noted that lateral banks constraining the floodplain of his experimental setup may have been important in the spacing of the vortices; in subaqueous channels, the flow is generally constrained laterally by a mobile barrier – the ambient fluid. As such, through time the location and strength of this barrier will vary, which would suggest that regular downchannel spacing of vortices may not be achieved in subaqueous channels.

Rotation of flow within these vortices may cause relatively rapid deposition as the reversed portion of the flow interacts with flow travelling in the ‘normal’ overspill direction. These observations of flow behaviour may explain the apparently counter-intuitive orientation of the outer-bend overbank ridges. The overbank depositional features are termed sediment waves based on observations from the inner-bend overbank area where the deposit crest-lines are formed perpendicular to interpreted stream-lines; the more complex geometries and orientation of the outer-bend waves can be explained by the formation of vortices and their interaction with other parts of the overspill. The more distal part of the outer-bend overbank deposit indicates a zone of flow divergence, with more minimal deposition occurring between the sediment waves with diverging crest orientations (Fig. 5).

### 3 SEDIMENT WAVE EVOLUTION

Ten nominally identical flows were run in the mid-depth channel model (ar8), with deposit profiles taken between each. As vortex formation is not a uniform event on the outer-bend overbank, there is considerable variation in depositional focus between

different flows. For that reason, the sediment waves on the inner-bend overbank, which appear to be deposited from flows which are more uniform in character, are focused upon here.

Deposition from successive flows formed sediment waves which amplified during the early stages of evolution, but were progressively ‘healed’ through deposition. Had the waves exhibited greater relief this may not have been the case. In addition, deposition within the channel occurred at a slightly greater rate than on the overbank leading to a slight successive increase in overbank flow volume between runs. A transect was taken through the inner-bend waves and the cross sections were measured (Figs. 1 & 6). The positions of the waves are clear on the deposit profiles and they appear to aggrade vertically, however, the profiles have significant vertical exaggeration, flattening the profiles reveals a component of upstream (i.e., towards the point of overspill) migration. The complex crest-line morphology of the waves becomes more uniform through time as they coalesce, eventually forming a compound deposit mirroring the curve of the channel.

#### 3.1 Discussion of sediment wave evolution

Two sediment wave deposition mechanisms are commonly cited; i) formation under antidune flow conditions which are assumed to lie within the subcritical to supercritical boundary (i.e., Froude number  $\sim 1$ ) (Allen, 1970; Normark et al., 1980; Wynn et al., 2000); ii) lee waves which associated with subcritical flows (i.e., Froude numbers  $< 1$ ) (e.g., Flood, 1988; Lewis & Pantin, 2002). Froude number calculations for the channelised part of the flow were in the region 0.6, overbank flow is slower than channelised flow (Fig. 2 & 3) so the presence of antidune conditions is ruled out, the alternative explanation may therefore be the formation of lee waves with a degree of upstream migration of the deposit (e.g., Flood, 1988). In their detailed study of sediment waves on the Var Fan, Migeon et al. (2000) found several styles of sediment wave evolution. Simple aggrading levees were found to be related to areas on the fan where channel-levees were high, preventing high energy spill-over; accordingly, in this experimental study there might be expected a greater degree of upslope migration of the waves as the confinement decreased due to intra-channel deposition, unfortunately this could not be reliably constrained with the data. The sediment waves illustrated here are relatively short-lived features, their intricate planforms are soon swamped by sedimenta-



tion; the key importance of these features was the recognition of complex flow behaviour during their deposition. The complexity of flow may be masked through time as deposition heals the wave topography to form approximately channel-parallel deposits

(levees). However, recognition of such flow behaviour may come from analysis of macroscopic palaeoflow indicators and also of grain-fabric within individual turbidites.

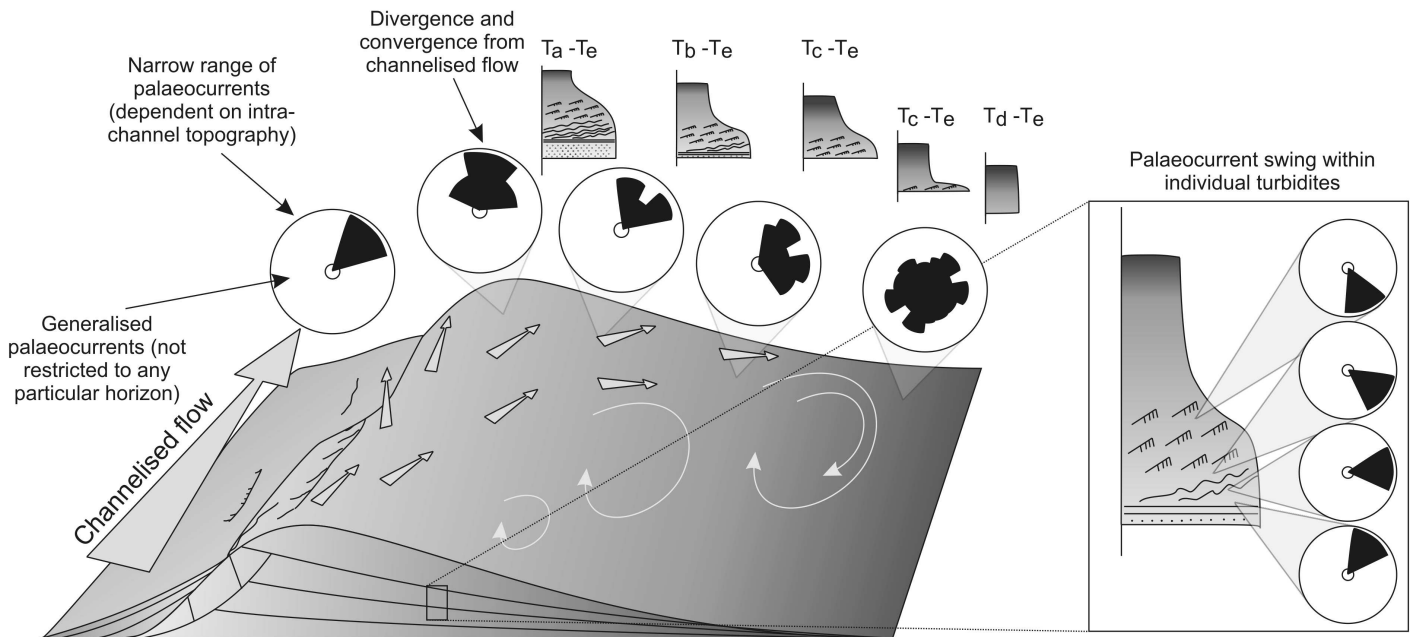


Figure 7. Summary diagram of the process of vortex formation on submarine channel-levees, and the origin of intra-bed palaeocurrent swing.

#### 4 DISCUSSION

Palaeocurrents within levee deposits may be complex. In the Cretaceous Rosario Formation palaeocurrents beyond the position of the inferred levee crest were divergent with the channel-axis, at a greater distance the palaeocurrents showed considerable scatter; this was attributed to the possible presence of topography (Kane et al., 2007). More typically a ‘chevron pattern’ of opposing palaeocurrents has been documented from ancient channel-levees (e.g., Hesse and Dalton, 1995); however, detailed palaeocurrent studies, especially intra-bed studies of grain-fabric, which may elucidate such behaviour, are generally lacking. In the levees of the Amazon Fan, using anisotropy of magnetic susceptibility to determine grain-fabric orientations, considerable ‘swing’ of palaeocurrents within individual turbidite beds was noted and attributed to “shifting patterns of meandering streamlines in the flow as deposition proceeds” (Hiscott et al., 1997, p. 64), based on some earlier work on turbidite beds displaying similar patterns of palaeocurrent swing (Parkash, 1970; Parkash and Middleton, 1970). Hiscott et al. (1997) suggest that this palaeocurrent swing may be imparted on the flow by levee topography but were not able to constrain this with their data. Parkash (1970) and Parkash and Middleton (1970) describe a down-

current increase in the ‘sinuosity’ of palaeocurrents within individual beds; additionally they noted the variation from more uni-directional palaeocurrents at the base of beds to a wider spread of palaeocurrents towards the tops of beds.

The formation of vortices provides an alternative explanation for the observed palaeoflow record in the ancient and more recent examples given above. Irregular levee topography could promote vortex formation but these experiments demonstrate that irregular topography is not necessary. A general conceptual model of overspill from a submarine channel levee is illustrated (Fig. 7). Converging overbank flow on the inner-bend resulted in sediment waves with crests approximately parallel to the channel bend; converging flow reinforces itself helping to maintain the overbank velocity, reducing the effects of lateral spreading and of shear stress exerted by the through channel flow. Hence it may be envisaged that strong overbank flow may produce more uniform overbank flow and deposits. In the proximal regions of a sinuous channel, where flows may be strongly overspilling, palaeocurrents may be more unidirectional. Flows may reach an equilibrium state with their cross-sectional geometry through the process of overspill in more proximal locations (e.g., Kane et al., 2008; Straub et al., 2008), therefore, overspill may be

much reduced in distal areas potentially resulting in more complex overbank flow behaviour and resultant palaeocurrents.

## 5 CONCLUSIONS

i) Overbank flow behaviour may be complex through the generation of vortices and increased turbulence at channel margins; this was recognised from the deposition of sediment waves with intricate morphologies.

ii) Resultant deposits, in particular grain-fabrics within individual turbidites, may reflect this complex behaviour.

iii) As overspill and turbulence/vorticity generation may be non-uniform, the compound overbank deposit (levee) will approximately track the overall channel planform. Sediment waves may reflect vortex formation in situations where the formation of vortices occurs repeatedly through time, e.g., at a channel outer-bend in a system dominated by flows that fall within a narrow range of volumes.

iv) Vortex formation bears a similarity of process to that of vortex formation in flooded fluvial channels but also bears a resemblance to atmospheric flows encountering topography.

## 6 ACKNOWLEDGEMENTS: I

IK and WDM are funded through Phase 5 of the Turbidites Research Group. We thank Gareth Keevil for laboratory assistance.

## 7 REFERENCES

- Alavian, V. & Chu, V. H. 1985. Turbulent exchange flow in shallow compound channels. Proceedings of the 21<sup>st</sup> International Congress of IAHR, Melbourne, 446-451.
- Allen, J. R. L. 1970. Physical processes of sedimentation. George Allen & Unwin Ltd, London. 248pp.
- Barishnikov, N. B., Ivanov, N. B. & Sokolov, U. N. 1971. Role of the floodplain in flood of a river channel. Proceedings of the 14th Congress of the IAHR, Paris, Vol. 5, p. 141-144.
- Best, J. L., & Ashworth, P., 1994, A high resolution ultrasonic bed profiler for use in laboratory flumes: Research methods Papers, p. 674-675.
- Best, J. L., Kirkbride, A., & Peakall, J. 2001. Mean flow and turbulence structure of sediment-laden gravity currents: new insights using ultrasonic Doppler velocity profiling. In McCaffrey, W.D., Kneller, B. C., and Peakall, J., eds., *Particulate Gravity Currents; Special Publication of the International Association of Sedimentologists*, v. 31, p. 159-172.
- Bousmar, D. & Zech, Y. 1999. Momentum Transfer for Practical Flow Computation in Compound Channels. *Journal of Hydraulic Engineering*, 125, 696-706.
- Eaton, B. C. & Church M. 2004. A graded stream response relation for bed load dominated streams: *Journal of Geophysical Research - Earth Surface*, v. 109, doi:10.1029/2003JF000062.
- EEZ-Scan 84 Scientific Staff. 1988. Physiography of the western United States Exclusive Economic Zone, *Geology*, v. 16, p. 131-134.
- Flood, R.D. 1988. A lee wave model for deep-sea mudwave activity. *Deep-Sea Research*, v. 35, p. 973-983.
- Fukuoka, S. & Watanabe, A. 1995. Horizontal flow structure in channels with dense vegetation clusters and the numerical analysis thereof. Proceedings of the 27<sup>th</sup> Congress of the IAHR.
- Fukuoka, S. & Watanabe, A. 1997. Horizontal structures of flood flow with dense vegetation clusters along main channel banks. Proceedings of the 27<sup>th</sup> Congress of the IAHR.
- Graf, W. H. 1971. Hydraulics of sediment transport. McGraw-Hill, New York.
- Ikeda, S., Kawamura, K., Toda, Y., & Kasuya, I. 2002. Quasi-three-dimensional computation and laboratory tests on flow in curved compound channels. Proc., Riverflow 2002, Louvain-la-Neuve, Belgium, 233-245.
- Kane, I. A., Kneller, B. C., Dykstra, M., Kassem, A. & McCaffrey, W. D. 2007. Anatomy of a submarine slope channel-levee; an example from Upper Cretaceous slope sediments, Rosario Formation, Baja California, Mexico. *Marine and Petroleum Geology*, p. 540-563.
- Kane, I. A., McCaffrey, W. D. & Peakall, J. 2008. Controls on sinuosity evolution in submarine channels. *Geology*.
- Kenyon, N.H., Amir, A., & Cramp, A. 1995. Geometry of the younger sediment bodies of the Indus Fan. In Pickering, K.T., Hiscott, R.N., Kenyon, N.H., Lucchi, F.R., Smith, R.D.A., eds., *Atlas of Deep-water Environments: Architectural Styles in Turbidite Systems*. Chapman and Hall, London, pp. 89-93.
- Klaucke, I., Hesse, R. & Ryan, W.B.F. 1997. Flow parameters of turbidity currents in a low-sinuosity giant deep-sea channel: *Sedimentology*, v. 44, p. 1093-1102.
- Knight, D. W. & Shiono, K. 1990. Turbulence measurements in a shear layer region of a compound channel. *Journal of Hydraulic Research*, v. 28(2), 175-195.
- Knight, D. W., Yuen, K. W. H., & Al-Hamid, A. A. I. 1994. Boundary Shear Stress Distributions in Open Channel Flow, In Beven, K. J., Chatwin, P. C., and Millibank, J. H., eds., *Mixing and Transport in the Environment*, Wiley, Chichester, pp.51-87.
- Kolla, V., Bourges, P., Urrity, J.M., & Safa, P. 2001. Evolution of deep-water Tertiary sinuous channels offshore Angola (west Africa) and implications for reservoir architecture: *Bulletin of the American Association of Petroleum Geologists*, v. 85, p. 1373-1405.
- Leeder, M. R. 1982. *Sedimentology, Process and Product*: George Allen and Unwin Publishers, London, pp. 344.
- Lewis K. B. & Pantin, H. M. 2002. Channel-axis, overbank and drift sediment waves in the southern Hikurangi Trough, New Zealand. *Marine Geology*, 192, 123-151.
- Migeon, S., Savoye, B., Zanella, E., Mulder, T., Faugères J-C. & Weber O. 2001. Detailed seismic and sedimentary study of turbidite sediment waves on the Var sedimentary ridge (SE) France: significance for sediment transport and deposition and for the mechanism of sediment wave construction. *Marine and Petroleum Geology*, 18, 179-208.
- Myers, W.R.C. & Brennen, E.K. 1990. Flow Resistance in a Compound Channel, *Journal of Hydraulic Research*, 28, 141-146.

- Nadaoka, K., & Yagi, H. 1998. Shallow-water turbulence modeling and horizontal large-eddy computation of river flow. *Journal of Hydraulic Engineering*, 124, 493–500.
- Naish, C. & Sellin, R. H. J. 1996. Flow structure in a large-scale model of a doubly meandering compound river channel. In: P. J. Ashworth, S. J. Bennet, J. L. Best, and S. J. McLelland, eds., *Coherent flow structures in open channels*. Wiley, Chichester, England, p. 631-654.
- Nokes, R. L & Hughes, G. O. 1994. Turbulent mixing in uniform channels of irregular crosssection. *Journal of Hydraulic Research*, 32 (1), 67-86.
- Normark, W.R., Hess, G.R., Stow, D.A.V. & Bowen, A.J. 1980. Sediment waves on the Monterey Fan levee: a preliminary physical interpretation. *Marine Geology*, 37, p. 1-18.
- Parkash, B. 1970. Downcurrent changes in sedimentary structures in Ordovician turbidite greywackes. *Journal of Sedimentary Research*, 40, 572-590.
- Parkash B. & Middleton, G.V. 1970. Downcurrent textural changes in Ordovician turbidite graywackes. *Sedimentology*, 14, 259–293.
- Peakall, J., Ashworth, P., & Best, J. 1996. Physical modelling in fluvial geomorphology: principles, applications and unresolved issues, in Rhoads, B. L., and Thorn, C. E., eds., *The Scientific Nature of Geomorphology*. John Wiley and Sons, Chichester, p. 221-253.
- Peakall, J., McCaffrey, W.D., & Kneller, B.C., 2000, A process model for the evolution, morphology and architecture of meandering submarine channels: *Journal of Sedimentary Research*, v. 70, p. 434-448.
- Peakall, J., Ashworth, P. J. & Best, J. L. 2007. Meander-bend evolution, alluvial architecture and the role of cohesion in sinuous river channels: a flume study. *Journal of Sedimentary Research*, v. 77, p. 197-212.
- Pirmez, C., and Imran, J., 2003, Reconstruction of turbidity currents in Amazon Channel: *Marine and Petroleum Geology*, v. 20, p. 823-849.
- Prooijen, B. C, Battjes, J. A. & Uijtewaal, W. S. J. 2005. Momentum Exchange in Straight Uniform Compound Channel Flow, *Journal of Hydraulic Engineering*, 131, 175-183.
- Rowinski, P. M., Czernuszenko, W., Koziol, A. P. & Kubrak, J. 2002 Properties of a streamwise turbulent flow field in an open two-stage channel, *Archives of Hydro Engineering and Environmental Mechanics*, 49 (2), 37-51.
- Rowiński, P. M., Czernuszenko, W. & Krukowski, M. 2005. Migration of Floating Particles in a Compound Channel. In: Czernuszenko, W. and Rowiński, P. M., eds., *Water Quality Hazards and Dispersion of Pollutants*. Springer US, p. 121-141.
- Schumm, S.A., Mosley, M.P., & Weaver, W.E. 1987. *Experimental Fluvial Geomorphology*. New York, John Wiley & Sons, 413 p.
- Sellin, R. H. J. 1964. A laboratory investigation into the interaction between flow in the channel of a river and that over the flood plain. *Houille blanche*, 7, 793-801.
- Shiono, K. & Knight, D. W. 1991. Turbulent open channel flows with variable depth across the channel. *Journal of Fluid Mechanics*, 222, 617-646.
- Shiono, K., Scott, C. F. & Kearney, D. 2003. Predictions of solute transport in a compound channel using turbulence models. *Journal of Hydraulic Research*, 41(3), 247-258.
- Shiono, K. & Feng, T. 2003. Turbulence measurements of dye concentration and the effect of the secondary flow on its distribution in open channel flows, *Journal of Hydraulic Engineering*, 129 (5), 373-384.
- Sofialdis, D. & Prinos, P., 1999. Turbulent flow in open channels with smooth and rough floodplains. *Journal of Hydraulic Research*, 37(5), 615-640.
- Straub, K.M., Mohrig, D.C., Buttles, J., McElroy, B., & Pirmez, C. 2008. Interactions between turbidity currents and topography in aggrading sinuous submarine channels: a laboratory study: *Geological Society of America Bulletin*.
- Tal, M. & Paola, C. 2007. Dynamic single-thread channels maintained by the interaction of flow and vegetation. *Geology*, v. 35, p. 347-350.
- Tamai, N., Asaeda, T., Ikeda, Y. 1986. Study on generation of periodical large surface eddies in a composite channel flow. *Water Resources Research*, 22, 1129-1138.
- Wood, I. R., & Liang, T. 1989, Dispersion in an open channel with a step in the cross-section, *Journal of Hydraulic Research*, 27(5), 587-601.
- Wynn, R. B., Masson, D. G., Stow, D. A. V., & Weaver, P. P. E. 2000a. Turbidity current sediment wave on the submarine slopes of the western Canary Islands. *Marine Geology* 163, 185-198.
- Zheleznyakov, G.V. 1971. Interaction of Channel and Floodplain Flows. Proceedings of the 14th International Congress of IAHR, Paris, 144-148.